

VLBI Observations of a Complete Sample of Radio Galaxies VIII - Proper Motion in 3C338

G. Giovannini¹

Istituto di Radioastronomia, via Gobetti 101, 40129 Bologna, ITALY

W.D. Cotton

N.R.A.O., 520 Edgemont Rd, Charlottesville VA 22903-2475, USA

L. Feretti

Istituto di Radioastronomia, via Gobetti 101, 40129 Bologna, ITALY

L. Lara

Instituto de Astrofísica de Andalucía, CSIC, Apartado 3004, 18080, Granada, SPAIN

and

T. Venturi

Istituto di Radioastronomia, via Gobetti 101, 40129 Bologna, ITALY

Astrophysical Journal Vol. 493 - Feb. 1 1998 - in press

preprint n.: BAP 09-1997-027 IRA; available in: <http://boas3.bo.astro.it/bap/BAPhome.html>

ABSTRACT

We present new VLA, MERLIN and VLBI images for the radio galaxy 3C 338, and the results of the monitoring of its arcsecond core flux density. Present high sensitivity observations allow us to investigate the radio structure of this source and to confirm the presence of two symmetric parsec scale jets. Morphological changes between different epochs are evident and a proper motion with $\beta \sim 0.4h^{-1}$ has been derived allowing us to give a lower limit constraint for the Hubble constant. While the steep spectrum large scale structure of 3C 338 could be a relic emission, the small scale structure looks young, similar to the high power MSOs found at high redshift.

Subject headings: Galaxies: Nuclei — Galaxies: Jets — Galaxies: Individual (3C338) — Radio Continuum: Galaxies — techniques: interferometric, VLBI

¹Dipartimento di Astronomia, via Zamboni 33, 40126 Bologna, ITALY

1. Introduction

The radio galaxy 3C338 is classified as a FR I radio source (see Fanaroff and Riley, 1974 for the FR I definition) and shows central optical [OIII] line emission (Fisher et al., 1995). It has the steepest radio spectrum at cm wavelength of any 3CR source except 3C318.1 (Feretti et al. 1993). It is associated with the multiple nuclei cD galaxy NGC6166 at the center of the cooling flow cluster of galaxies A2199. Lucey et al. (1991) found for this cluster a peculiar velocity not significantly different from zero, therefore we derive its distance from the measured cluster redshift $z = 0.03023$ (Zabludoff et al., 1993).

Short exposure plates by Minkowski (1961) and Burbidge (1962) showed that the cD core consists of 4 separate optical components, with the brightest one coincident with the radio core. This complex structure is confirmed in a recent HST image (Capetti private communication).

In the low resolution radio maps, 3C338 shows a total extension of $\sim 2'$ with a core emission and 2 symmetric lobes slightly misaligned with respect to the core. High resolution radio maps (Burns et al., 1983) reveal the presence of a peculiar jet like filament within the extended structure of 3C338, but detached and significantly offset to the south of the compact radio core. This feature has a very steep spectrum as the entire diffuse structure does.

Burns et al. (1983) suggested two possible explanations for this peculiar structure: a) the ram pressure of a highly asymmetric cooling flow onto the cD galaxy; b) the motion of the radio core within the cD galaxy. If the radio core stopped its activity at some time and moved from its position, it could have left a steep spectrum aged radio jet behind. More recent observations (Ge et al. 1994) also identified a weak radio emission from the second optical nucleus of NGC 6166 and revealed faint symmetric jets on both sides of the 3C338 core, with a size of about $15''$. These new observations show also high RM values, ranging from -2000 to $+2000$ rad m $^{-2}$ in the two extended lobes, in the jet-like filament and also in the east jet. No polarized emission was detected from the core. The variation of polarization angles imply the existence of a screen in front of the radio source. A strong, ordered magnetic field with a dense medium in the center of a cooling flow could account for the observed results. In a recent paper Owen et al., (1997) using new ROSAT HRI X-ray data showed that the condi-

tions in the central regions of 3C338 are very complex. The strong cooling flow is not symmetric. They suggest that the conditions in the central cooling core could have disrupted the radio jet and created the low brightness emission. In this scenario, the bright emission south of the core is a high-emissivity transient filament, currently overpressured, for instance due to strong turbulence in the region. The short-scale radio jets found by Ge et al. (1994) would be a new, young radio emission from 3C338 which is now in a radio-active phase.

At parsec resolution, this source was first mapped by Feretti et al. (1993), who also pointed out that the arcsecond core radio emission is strongly variable. They obtained a high resolution VLBI map showing a central dominant core emission with a symmetric two-sided jet structure. This structure is aligned within 5° of the arcsecond jet structure found by Ge et al. (1994) on both sides of the arcsecond core. The parsec-scale symmetric structure can be formed by jets either moving at high velocity in the plane of the sky or with a non-relativistic speed.

In this work, we present new data obtained with the Very Large Array (VLA), the Multi-Element Radio Linked Interferometer Network (MERLIN) and the Very Long Baseline Interferometer (VLBI), for a detailed study of this peculiar source and a discussion of its core radio properties. We use a Hubble constant $H_0 = 100$ km sec $^{-1}$ Mpc $^{-1}$ therefore at the distance of 3C338, 1 mas corresponds to 0.41 pc.

2. Observational Data

2.1. VLA Data

2.1.1. Monitoring of the arcsecond core flux density

We observed the arcsecond core radio emission of this source with the VLA in the A-array configuration at different frequencies in order to derive the arcsecond core flux density. The source was observed for about 10 minutes at each frequency at different hour angles to obtain a better uv-coverage. The data have been calibrated in the standard way using the Astronomical Image Process System (AIPS) and have been reduced using the MX or IMAGR AIPS tasks. The core flux density was obtained by fitting an elliptical Gaussian to the nuclear source (IMFIT). Our data set includes also VLA data when the VLA was used as a phased array during VLBI observations. In addition, literature data and unpublished VLA archive

data were used. The flux density monitoring data are shown in Table 1 and in Fig. 1. The arcsecond core source has shown 2 main flares about 15 years apart and is now in a low state. Unfortunately, we have no high frequency data in the time range 1980 - 1990 therefore we cannot exclude the possibility that the core has had more flares in this period. Comparing data at the same epoch, the spectral index of the arcsecond core turns out to be $\alpha \sim 0.3$ between 1.4 and 8.4 GHz ($S(\nu) \propto \nu^{-\alpha}$).

2.1.2. VLA maps

High quality images of 3C338 at the arcsecond resolution were obtained from the long VLA observations made as part of the VLBI sessions as a phased array. In Fig. 2a we present the VLA map obtained at 1.7 GHz with the VLA in the VLBI session on 1991 June 18. It was deconvolved using the Maximum Entropy Method (AIPS task VTESS) which shows in better detail the low brightness extended regions. The nuclear source has been partially subtracted. The central region is easily visible with two symmetric, short jets which end in faint hot spots. The radio structure of this small region is similar to that of extended FR II radio galaxies but on a much smaller scale.

The extended low brightness region as well as the peculiar jet-like filament structure are evident in Fig. 2a. The filament structure is visible beyond the west lobe. In Fig. 2b, we have superimposed the radio map onto the optical image taken from a CCD frame in the V band made with the 2.1 m reflector at San Pedro Martir (Baja California) belonging to the Osservatorio Astronomico Nacional de Mexico, and kindly provided by G. Gavazzi (see Gavazzi et al. 1995 for details). The optical image shows the three main optical nuclei of 3C338 (the fourth, being very weak, is barely visible as a small extension to the east of the northern one). The radio emission is identified with the dominant optical nucleus which is more diffuse, but with a bright unresolved optical emission coincident with the radio core. The two secondary nuclei are more compact with a bright central emission.

In Fig. 3 we show the core region at 5.0 GHz from VLA data obtained in the VLBI session on 1995 September 11. The VLA was in the A/B configuration with most of the telescopes in the B configuration; therefore, the resolution of this map is very similar to that presented in Fig. 2. The core source is the dominant feature of this small size structure. Two barely resolved symmetric jets connect the core to the

Table 1: Arcsecond core flux densities

Epoch Mon. Year	$S_{1.4GHz}$ mJy	S_{5GHz} mJy	$S_{8.4GHz}$ mJy	Ref.
Dec. 1974	—	164	—	5
Feb. 1975	—	150	—	5
Dec. 1975	—	150	—	5
Aug. 1976	—	149	—	5
Jan. 1977	—	149	—	5
May 1978	—	130	—	5
Feb. 1980	—	115	—	5
May 1980	153	105	—	1
Sep. 1982	159	—	—	2
Dec. 1984	146	—	—	3
Apr. 1989	—	154	—	6
Apr. 1990	—	168	143	7
Mar. 1991	—	—	136	4
June 1991	181	—	—	4
Aug. 1991	—	158	127	4
Jan. 1993	184	140	—	4
Apr. 1994	167	111	93	4
Nov. 1994	—	113	87	4
Sep. 1995	—	111	87	4
Oct. 1995	163	—	—	4

REFERENCES.— 1: Burns et al., 1983; 2: Parma et al., 1986; 3: de Ruiter et al., 1986; 4: present paper; 5: Ekers et al., 1983; 6: Ge p.c.; 7: Feretti et al., 1993.

two hot spots, where the radio structure seems to terminate. Both hot spots are resolved and their deconvolved size is 0.8" (0.33 Kpc - East one) and 1.4" (0.57 Kpc - West one). No connection between this central radio emission and the extended steep spectrum low brightness emission is visible. The distance between the core and the eastern and western hot spots is 6.4" (3.0 kpc) and 6.0" (2.8 kpc), respectively. The properties and shape of this structure appear to resemble Compact Symmetric Sources (see Sect. 3.4).

We confirm the existence of the faint radio emission from the second optical nucleus (Ge et al. 1994) with a flux density of ~ 0.5 mJy at 5 GHz (figure not presented here). We did not attempt to study the polarized emission since we do not have the frequency coverage necessary to study this high RM source, and refer to Ge et al. (1994) for a detailed polarization study of 3C338.

We used the 1.7 and 5.0 GHz data to derive a spectral index map of the extended structure of 3C338 at arcsecond resolution (not shown here), the uv-coverage of the two datasets being very similar. The structure in the central region has a moderately steep spectrum ($\alpha = 0.7 - 1.5$ in the two symmetric jets; $\alpha = 1.1$ in the two hot spots), while the detached extended lobes and the relic jet structure have a very steep spectrum ($\alpha = 1.7 - 3.0$), in agreement with Burns, (1983).

2.2. MERLIN Data

We observed 3C338 with the MERLIN array on 1995 October 29 at 1.66 GHz with a 15 MHz bandwidth for 12 hours. We used the following telescopes: Defford, Cambridge, Knockin, Wardle, Darnhall, MK2, Tabley. The data were edited and amplitude calibrated in Jodrell Bank using the standard procedure based on the OLAF programs. 3C286 was used as amplitude calibrator. The data were then written in FITS format and loaded into AIPS where the phase calibration using standard MERLIN phase calibrators was carried out. The source was then mapped and the data self-calibrated following the standard procedure. In Fig. 4 we present the MERLIN map obtained using *Natural* weighting. The large scale structure is completely resolved and the filament jet-like structure to the south of the core shows a uniform distribution with no evidence of unresolved knots inside. The core is easily visible with a few sidelobes due to dynamic range problems. Some indication of the two short symmetric jets is present and

the eastern hot spot is marginally resolved while the western one is completely resolved. At the highest resolution (uniformly weighted map, HPBW = 130 mas) only a slightly resolved core (~ 30 mas in size) is visible.

No polarized flux has been detected in the MERLIN data at a level of 0.1 mJy/beam.

2.3. VLBI Data

Table 2 summarizes the VLBI observations which are presented in the following sub-sections. The noise level and angular resolution (HPBW) are given for natural weighted maps.

2.3.1. Data at 1.7 GHz

We observed 3C338 at 1.7 GHz on 1991 June for 12 hours with the MK3 mode B recording system (28 MHz bandwidth) with the following global array: Bonn, Jodrell MK1, Medicina, Onsala, WSRT, Green Bank, Haystack, VLBA-Owens Valley and Pie Town. Standard amplitude calibration was done using the system temperature method in AIPS. Data were then globally fringe fitted and self-calibrated in the standard way. We made 6 iterations of phase self-calibration and 1 phase+gain to produce the final map shown in Fig. 5. The source shows a central component that we identify with the nuclear source and a symmetric structure extended about 30 mas to the east and 20 mas to west. The faint, more diffuse emission visible to the west at 40 mas from the core is probably real. The size and position angle of the symmetric structure is in agreement with the "core" parameters derived from the full resolution MERLIN map.

2.3.2. Data at 5 GHz

At 5 GHz 3C338 was mapped by us for the first time in 1989 September (see Feretti et al., 1993), and observed again on 1994 November and 1995 September with the full VLBA + the phased VLA. The observations were carried out switching every 30 minutes from 5 to 8.4 GHz obtaining two maps at two observing frequencies at the same epoch and with good uv-coverage. The data have been correlated in Socorro. The parsec scale structure shows a central dominant feature (the core emission) and two symmetric jets. The eastern jet is slightly stronger and longer (Fig. 6). The eastern jet shows a couple of low brightness regions in its center suggesting it could be

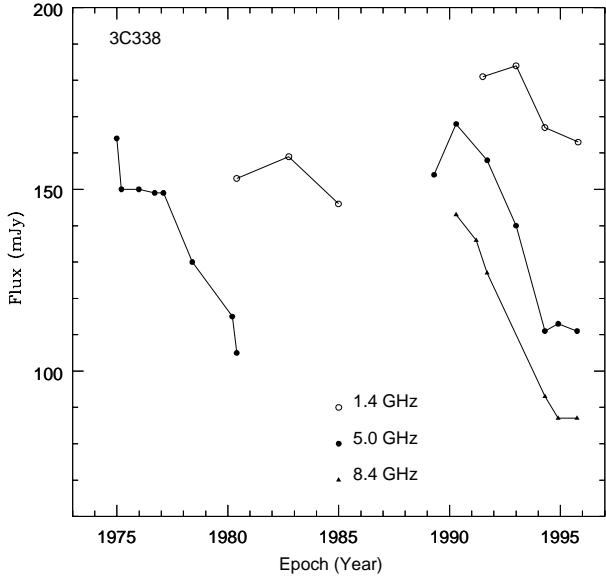


Fig. 1.— Flux density measures of the 3C338 arc-second core. Connection lines are for display use only and not a best fit. References to the different measures are given in Table 1.

Table 2: VLBI maps

Frequency GHz	Array	Obs. data	HPBW mas	noise mJy/b
1.7	Global	Jun91	8.2×3.9	0.06
5.0	Global	Sep89	3.2×3.2	0.3
5.0	VLBA+Y	Nov94	3.2×3.2	0.2
5.0	VLBA+Y	Sep95	3.5×2.7	0.25
8.4	Global	Mar91	2.0×1.0	0.09
8.4	VLBA+Y	Nov94	2.2×2.2	0.15
8.4	VLBA+Y	Sep95	2.1×1.9	0.1

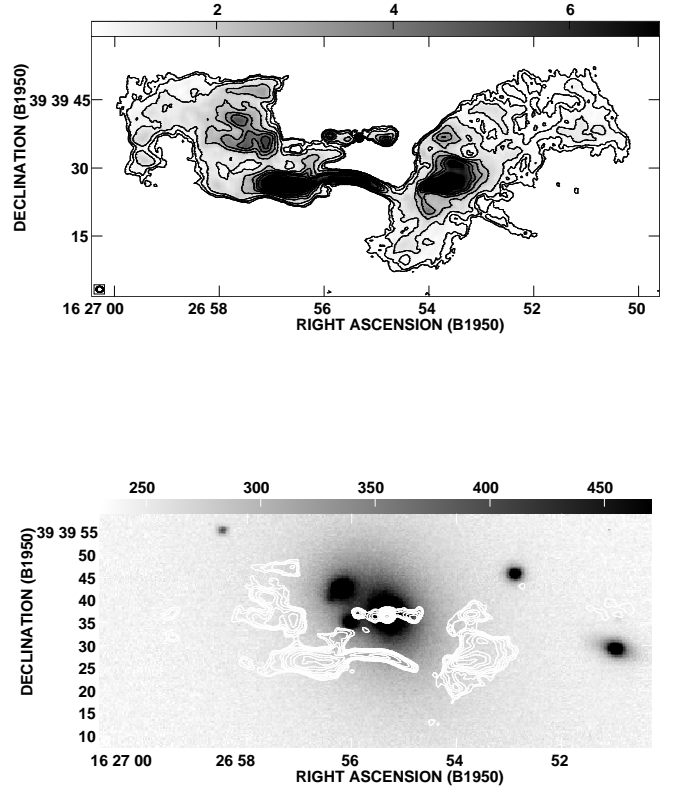


Fig. 2.— a- VLA map of 3C338 at 1.7 GHz deconvolved with the Maximum Entropy Method. The nuclear source has been partially subtracted. The HPBW is $1.42'' \times 1.28''$ in PA 84° and the noise level is 0.08 mJy/beam. Contour levels are: 0.4 0.6 1 2 3 4 5 7 10 mJy/beam. b- Optical CCD map of 3C338 (grey levels) super-imposed with the 1.7 GHz radio map (contour levels).

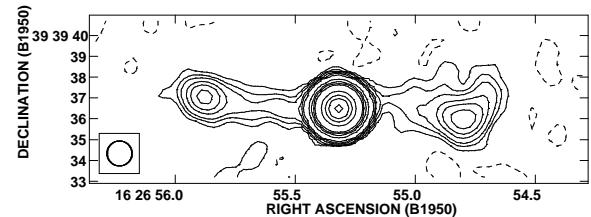


Fig. 3.— Isocontour map of the central region of 3C338 obtained with the VLA at 5.0 GHz. The HPBW is $1.2''$ and the noise level is 0.04 mJy/beam. Contour levels are: -0.1 0.1 0.2 0.3 0.5 0.7 1 3 5 7 10 30 50 70 100 mJy/beam.

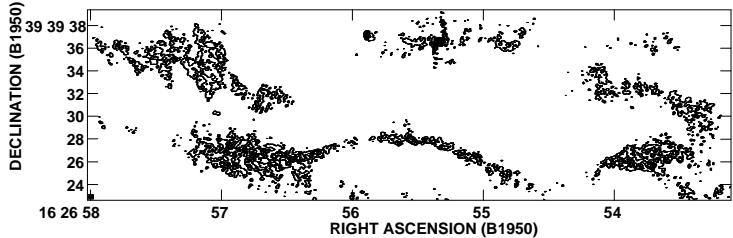


Fig. 4.— Isocontour map of 3C338 at 1.7 GHz obtained with the MERLIN array. The HPBW is 250 mas and the noise level is 0.13 mJy/beam. Contour levels are: 0.25 0.5 0.75 1 3 5 10 30 50 100 150 mJy/beam.

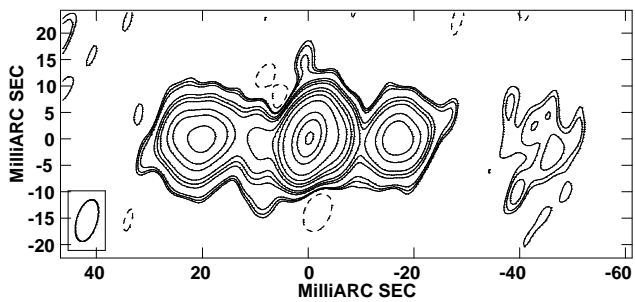


Fig. 5.— VLBI map of 3C338 at 1.7 GHz. The HPBW is 8.2×3.9 mas in PA -17° . The noise level is 0.06 mJy/beam. Contour levels are: -0.15 0.12 0.15 0.2 0.5 0.7 1 2 3 5 10 30 50 80 mJy/beam.

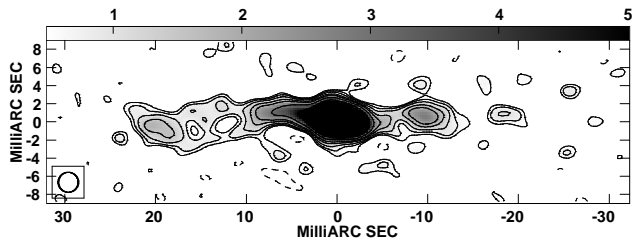


Fig. 6.— Isocontour map of 3C338 obtained with VLBA + Y27 at 5 GHz on November 1994. The HPBW is 2.2 mas and the noise level is 0.2 mJy/beam. Contour levels are: -0.5 0.5 0.7 1 1.5 2 3 5 10 30 40 mJy/beam

limb-brightened. Unfortunately, the 1995 data were seriously affected by the lack of data on the calibrator source due to technical problems and by the failure of some telescopes. Therefore these data produced a low quality map which does not add any useful detailed information about the source structure.

2.3.3. Data at 8.4 GHz

We observed 3C338 at 8.4 GHz on March 1991 with the following array: Bonn, Medicina, Noto, Onsala, Green Bank, Haystack, OVRO, VLA (phased array), VLBA-Pie Town and Kitt Peak. The data have been correlated in Bonn. Second and third epoch maps were obtained with the full VLBA + VLA phased array at the same time as the 5 GHz maps (see above). The 3 epoch maps are given in Fig. 7. At 8.4 GHz the source is symmetric, but the eastern jet is somewhat longer and brighter than the western jet. The central component is dominant in all maps, however it shows a clear change of structure in the 3 epochs.

3. Discussion

3.1. Changes in the pc scale structure and proper motion

With the VLBI observations at our disposal, we performed a multi-epoch morphological comparison of 3C338.

At 8.4 GHz, the morphological change between different epochs is quite evident (Fig. 7). In particular, the map of the first epoch is dominated by a single central component of high brightness, while the more recent observations show two resolved components in the core region. Moreover, there are slight changes in the location and position angle of the blobs. The maps at 5 GHz are consistent with this change of structure, although their resolution is lower.

To better enhance the structural variations, we produced slices of the brightness along the ridge of maximum brightness, in the innermost region, i.e. where the brightness is higher (see Fig. 8). The alignment of the first and second epoch map is not unique, therefore we distinguish the following possible cases.

Case 1. The central peak in the first epoch map coincides with the true core and the two central components detected in the second and third epoch are new ejecta, separated by 1.5 mas, with the true core in between (see Fig. 8). The central structure detected in the first epoch is slightly resolved (~ 1.5

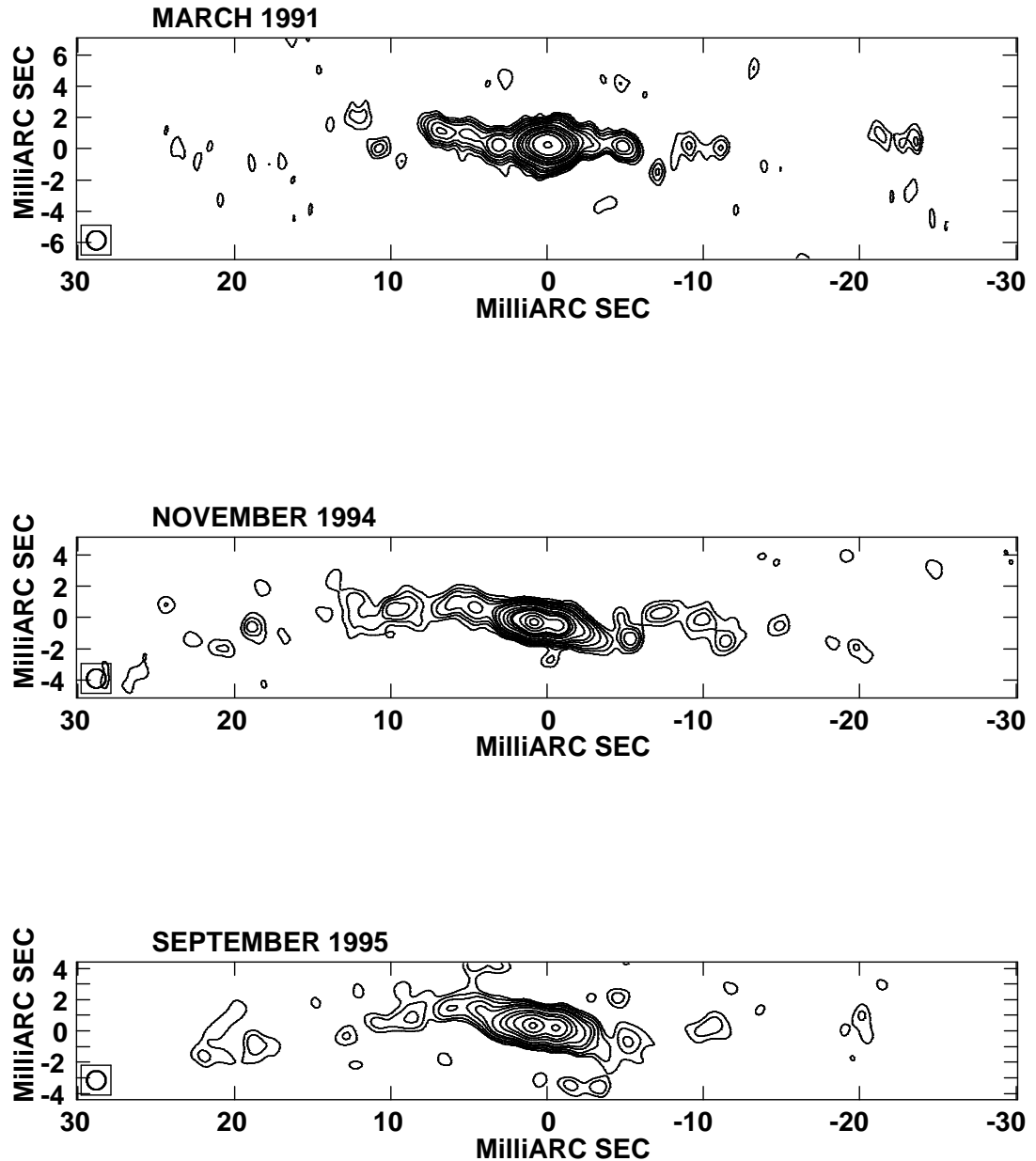


Fig. 7.— Multi epoch maps of 3C338 at 8.4 GHz. The peak flux is 64.0 mJy/beam for the first epoch map (top), 27.1 mJy/beam for the second epoch map (middle) and 21.0 for the third epoch map (bottom). For all the maps, the HPBW is 1.2 mas and contour levels are: 0.5 0.7 1 1.5 2 3 5 7 10 15 20 30 60 mJy/beam.

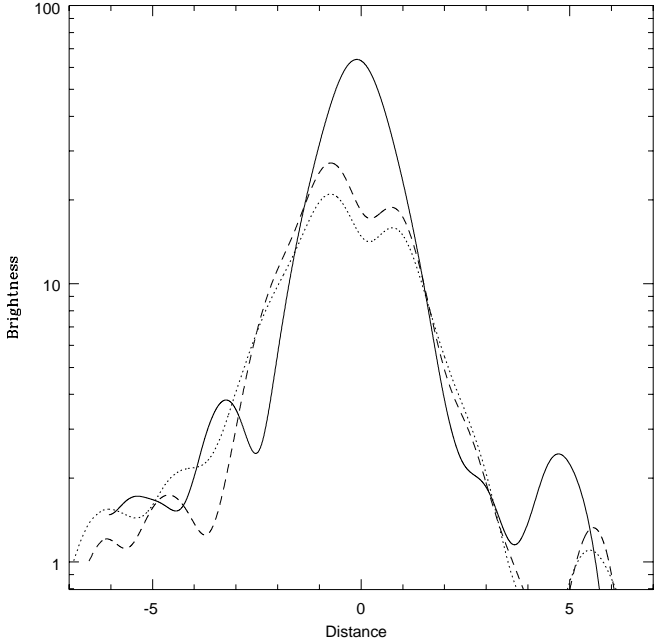


Fig. 8.— Overlay of the brightness of the 3 epochs, assuming that the core is between the two component detected in the second and third epoch. The continuous, dashed and dotted lines refer to the first, second and third epoch, respectively.

mas) and could be produced by a double source, with point-like identical components, of separation ~ 1.25 mas. Therefore, the new ejecta have moved of at least 0.12 mas between the first and second epoch. A larger proper motion is seen in three outer blobs. Since the blobs are weak, they could be affected by positional uncertainties related with the application of the clean algorithm. On average, we estimate that each blob has moved away from the core of about 1.1-1.2 mas between the two epochs. This leads to an apparent blob velocity $\beta_{app} = 0.41h^{-1} - 0.45h^{-1}$, ($h = H_0/100$) which corresponds to a true velocity $\beta > 0.38h^{-1} - 0.41h^{-1}$. The apparent blob velocity is consistent with the lack of proper motion between the second and third epoch. In fact, the implied displacement of the blobs between the two observations should be 0.23-0.25 mas. The apparent velocity of the two symmetric innermost blobs is lower. Features moving at different velocities, as well as moving and stationary components are common in extragalactic radio sources (see e.g. Zensus et al., 1995). We will consider here as 3C338 proper motion the faster one, derived from the outer components.

Case 2. The easternmost strong peak detected in the second and third epoch contains the true core,

and coincides with the peak of the first epoch (Fig. 8). The motion of the blobs is very similar to that obtained in the previous case, but the emission is asymmetric and the blob motion too. A flip-flop mechanism could explain the two-sided morphology.

Case 3. The westernmost strong peak detected in the second and third epoch is the true core, while the easternmost one is a new component. In this case, the new component shows an apparent velocity $\beta = 0.63h^{-1}$, while the outer blobs seem stationary between the first and second epoch. An upper limit to their velocity of 0.1 c is obtained. If this is the case, the source is very peculiar, with a large velocity decrease of the blobs shortly after their ejection. Alternatively they could be stationary components due to a bend in the jet, although no large bend is present at pc and kpc resolution in this source. As in case 2, a flip-flop mechanism should be involved.

We consider the first possibility as the most reliable, because the two-sided ejection is what we expect given the large scale symmetry and because the two components show a similar behaviour in the flux density variation between the second and third epoch. Therefore, hereafter we will discuss only the case of

the symmetric emission.

3.2. Flux variability and spectrum

The morphological change discussed in the previous subsections is related to the variability of arcsecond core flux density. The first epoch map was made in a period of maximum flux density of the arcsecond core, while the second and third epochs are in a low flux density stage.

A comparison of the images obtained in November 1994 at 5 and 8.4 GHz indicates that the spectral index of the double source at the center is 0.4. The flux density of both components decreases from the second to the third epoch, by almost the same amount (15-20%). This similar behaviour reinforces the interpretation that the two components are two ejected blobs, moving away from the core. Their flux density variation could be related to adiabatic expansion during the propagation. We also note that the strongest peak is the eastern one, i.e. on the same side of the main jet (Sects. 2.3.2 and 2.3.3).

We can therefore suggest that the high state of flux density in the arcsec core (see Fig. 1 and Table 1) is related to the emission of new components, while the following flux density decrease is related to the propagation and expansion of these components. The emission of the two central components visible in the second epoch map would be related to the high arcsecond core flux density measured in 1991.

3.3. Source orientation with respect to the line of sight

In Giovannini et al. (1994) and Lara et al. (1997), the jet velocity and orientation were derived from observational constraints. Here we obtain the jet orientation and velocity in the light of the better estimate of the jet to counter-jet brightness ratio and of the proper motion measure. The eastern jet appears to be the main one as it shows a higher brightness, it is visible to a larger distance from the core and it is on the same side of the more compact "VLA" hot spot (see Fig. 5 and Sects. 2.3.2 and 2.3.3). We have measured a jet/counter-jet (j/cj) ratio $R \sim 1.4$. Assuming a jet spectral index = 0.5, with the relation

$$R = \left(\frac{1 + \beta \cos \theta}{1 - \beta \cos \theta} \right)^{2+\alpha} \quad (1)$$

we obtain $\beta \cos \theta \sim 0.07$.

From equation (1) and from the relation between β and β_{app} :

$$\beta = \frac{\beta_{app}}{\beta_{app} \cos \theta + \sin \theta} \quad (2)$$

we have

$$\tan \theta = \frac{2\beta_{app}}{R^{1/(2+\alpha)} - 1} \quad (3)$$

Assuming $\beta_{app} = 0.43$ (see Sect. 3.2) we derive that the parsec scale structure of 3C338 is at $\sim 80^\circ$ with respect to the line of sight, the jet velocity is $\beta \sim 0.40$, and the corresponding Doppler factor δ is 0.99. A value of δ close to 1 means that the two jets are not strongly de-boosted.

Of course this result implies a bulk jet velocity of the same order of the velocity of the moving knots (pattern velocity). We cannot exclude a jet with a bulk velocity higher than the pattern one, however a high jet velocity implies in any case an angle near to the plane of the sky since we have symmetric jets. A jet velocity of 0.9c is possible at an angle of 86° with respect to the line of sight, but it implies $\delta = 0.47$ i.e. a strong de-boosting of the jet brightness. Therefore, either the 3C338 jets are very peculiar with a very high intrinsic brightness or δ has to be ~ 1 . Another possibility is to have jets slower than the moving knots. In this case no constraint can be given to their orientation with respect to the line of sight. In fact large as well as small angles are possible for jets with a low bulk velocity (see Giovannini et al., 1994).

In the light of the Ghisellini et al. (1993) result and of the general agreement in literature between the bulk and pattern velocity for superluminal sources we will consider here that in 3C338 the jet velocity is very similar to the velocity derived from the moving knots.

We have analyzed how the present results are affected by the choice of the Hubble constant. If H_0 is $50 \text{ km sec}^{-1} \text{ Mpc}^{-1}$ the jet velocity becomes $0.8c$ and $\theta \sim 85^\circ$. In this case the Doppler factor is 0.64 and the two sided jets are de-boosted. The intrinsic flux density of the parsec scale structure is a factor ~ 4.8 higher than the measured one and the radio power of the parsec scale structure at 5 GHz becomes $\sim 10^{24.5} \text{ W/Hz}$. Therefore, the present data are consistent with both $H_0 = 100$ and $H_0 = 50 \text{ km sec}^{-1} \text{ Mpc}^{-1}$ and only allow us to derive the H_0 lower limit: $H_0 \geq 40 \text{ km sec}^{-1} \text{ Mpc}^{-1}$.

We have also checked whether the previously obtained velocity and jet orientation can account for the different jet lengths visible in our VLA maps (see Sect.

2.1.2). If we assume that this difference is due to the different jet direction (the eastern jet is approaching us while the western one is receding), the ratio of projected distances from the core is given by:

$$\frac{Length_{approach}}{Length_{reced}} = \frac{1 + \beta \cos\theta}{1 - \beta \cos\theta} \quad (4)$$

Assuming a constant jet velocity, and an arm length ratio = 1.07, we derive $\beta \cos\theta \sim 0.03$ in good agreement with the value from the j/cj ratio. The lower value found from the arm length ratio is expected for a jet decelerating at increasing distance from the core.

3.4. Source structure

The overall structure of 3C338 consists of two features, with very different properties: an active region, which includes the core, two symmetric jets and two faint hot-spots at the jet ends, and a diffuse region, displaced to the south, showing a jet like filament and low-brightness extended emission. There is no visible connection between the symmetric jets and the diffuse feature, which is characterized by very steep spectrum, and is then likely to be an old relic radio emission.

The properties of the active structure (as flux variability, proper motion and so on; see previous sections) support the model of Burns et al. (1983) that this is a re-born young radio source. If the hot spot advance velocity in the surrounding medium is $\sim 0.02c$ (the 'fast' model in Readhead et al., 1996), the time necessary to reach the present size is 5×10^5 yrs. This value becomes 2.5×10^6 yrs if the 'slow' model (Readhead et al. 1996) is assumed. We note that this structure fits very well in the class of *medium size symmetric objects* (MSOs) defined by Readhead et al., (1996) and Fanti et al., (1995). The only discrepancy is that 3C338 is a nearby low power source while the Compact Symmetric Objects (CSOs) and the MSOs discussed by Readhead et al., (1996) and Fanti et al., (1995) are high redshift, high power objects. In the evolutionary scenario, these high power compact sources expand into FR II sources and are therefore considered the likely progenitors of this class of sources. The young radio source in 3C338 could be a low power MSO as 4C31.04 (Cotton et al., 1995) which we expect to grow into an extended FR I source. The two faint hot spots at the jet ends could represent the regions of interaction between the jets and the dense surrounding medium. The existence of *recurrent sources* is also suggested by O'Dea (1997) as

a possible scenario to explain the fraction of Gigahertz Peaked Sources (GPS) with extended emission. In fact, if the new phase of activity begins while the extended relic is still visible, this should provide a compact young source with an old extended emission. Unlike GPSs (O'Dea, 1996), 3C 338 is embedded in a strong cooling flow, which prevents adiabatic losses. Therefore the relic emission is still visible when the youngest emission has evolved into a MSO source.

The parsec scale jets are bright and well collimated up to ~ 30 mas (~ 12 pc) from the core. This is consistent with the extent of the nuclear source in the MERLIN map, and the structure in the VLBI 18 cm map. Beyond that distance, the jets become weaker, and are visible only in the VLA image and marginally detected in the low resolution MERLIN map. In analogy with the properties of 3C264 (Baum et al. 1997), a strong jet deceleration coupled with a rapid expansion which produces a strong brightness decrease because of adiabatic losses, could be present. The *decollimation* region occurs very close to the nuclear source (~ 12 pc) while in 3C264 the jet is well collimated up to $\gtrsim 200$ pc. This difference can be related to the low power *young* radio emission of 3C338 or to interaction with the outer medium. Unfortunately, because of the presence of many blobs/shocks in the 3C338 jets, it is inconclusive to model their brightness and opening angle, and to derive the trend of velocity (see Baum et al. 1997). Arc second scale jets visible in the VLA maps (see Fig. 3) seem to be intrinsically connected to the parsec scale jets. They are well aligned and have similar properties. In fact, on both scales, the eastern jet is slightly dominant over the western one.

It is important to note that, despite of the expected orbital motion of the multiple optical nuclei (Burns et al., 1983), the radio jet direction is stable in time: the PA of the restarted jet is very close to the PA of the jet-like filament in the relic emission and at the same PA of the extended structure.

Owen et al. (1997) found an asymmetric X-ray emission around 3C338. Since the X-ray emission is extended in the jet direction, they suggested that the radio jet is transferring momentum to the X-ray gas, pushing it out. This requires a radio jet direction constant in time. The authors also suggest that the arcsecond scale jet becomes unstable and disrupts severely at about the present position, because of the interaction with the surrounding medium. Their derived age for the jet structure is $\sim 17 \times 10^6$ yrs, larger

than that derived by us, using the Readhead et al. (1996) model, but not in conflict. A larger source age implies a jet advance speed lower than that derived by Readhead et al. (1996) for MSOs and this lower velocity could be once again related to the low power of 3C338 with respect to classical MSOs and to the dense 3C338 environment.

4. Conclusions

We have presented here new VLA, MERLIN and VLBI maps of the radio galaxy 3C 338. Moreover we have collected all the available data on its arcsecond core flux density. The source shows a strong flux density variability with at least two epochs of major activity in the range 1974 – 1995.

The VLA and MERLIN images show the presence of a core emission with two-sided jets disconnected from the large scale emission. The VLBI data confirm the existence of symmetric pc scale jets. The orientation of this structure appears to be very constant in time despite of the complex dynamic conditions present in the 3C338 central regions.

Comparing maps obtained at different epochs, a change in the pc scale morphology is well evident, and it is probably correlated with the arcsecond core flux density variability. The structural changes suggest the presence of a proper motion with $\beta \sim 0.4 \text{h}^{-1}$ on both sides of the core. This symmetric motion allow us to constrain the Hubble constant to $H_0 \geq 40 \text{ km sec}^{-1} \text{Mpc}^{-1}$.

These properties suggest that the extended emission in 3C 338 is a relic structure not related to the present nuclear activity, whose age is comparable with that of the high power and distant MSOs discussed by Fanti et al., (1995) and Readhead et al., (1996). The low power of this young emission is in agreement with its evolution in a FR I radio source while more distant MSOs are expected to evolve in FR II sources.

We thank Dr. R. Fanti for useful suggestions, Dr. M. Bondi, Dr. D. Dallacasa and Dr. C. Fanti for a critical reading of the manuscript. We thank the staffs at the telescopes for their assistance with the observations and the Bonn and Socorro correlator people for the absentee correlation of the data. The National Radio Astronomy Observatory is operated by Associated Universities, Inc., under contract with the National Science Foundation.

REFERENCES

Baum, S.A., O'Dea, C.P., Giovannini G., Biretta J., Cotton, W.D., de Koff S., Feretti L., Golombek D., Lara L., Macchetto F.D., Miley G.K., Sparks W.B., Venturi T., Komissarov S.: 1997 ApJ483, 178.

Burbidge, E.M.: 1962 ApJ136, 1134

Burns, J.O., Schwendeman, E., White, R.A.: 1983, ApJ271, 575

Cotton, W.D., Feretti, L., Giovannini, G., Venturi, T., Lara, L., Marcaide, J., Wehrle, A.E.: 1995 ApJ452, 605

Ekers, R.D., Fanti, R., Miley, G.K.: 1983, A.A. 120, 297

Fanaroff, B.L., Riley J.M.: 1974, MNRAS167, 31

Fanti C., Fanti R., Dallacasa D., Schilizzi R.T., Spencer R.E., Stanghellini C.: 1995 A&A302, 317

Feretti L., Comoretto G., Giovannini G., Venturi T., Wehrle A.E.: 1993, ApJ408, 446

Fisher, D., Illingworth, G., Franx, M.: 1995 ApJ438, 539

Gavazzi, G., Boselli, A., Carrasco, L.: 1995 A&AS112, 257

Ge, J., Owen, F.N.: 1994, AJ108, 1523

Ghisellini, G., Padovani, P., Celotti, A., Maraschi, L.: 1993 ApJ407, 65

Giovannini, G., Feretti, L., Comoretto, G.: 1990 ApJ358, 159

Giovannini, G., Feretti L., Venturi T., Lara L., Marcaide J., Rioja M., Spangler S.R., Wehrle A.E.: 1994 ApJ435, 116

Lara, L., Cotton, W.D., Feretti, L., Giovannini, G., Venturi, T., Marcaide, J.M.: 1997 ApJ474, 179

Lucey, J.R., Gray, P.M., Carter, D., Terlevich, R.J.: 1991 MNRAS248, 804

Minkowski R.: 1961 AJ66, 558

O'Dea, C.P.: 1996 Proceedings of the Second Workshop on Gigahertz Peaked Spectrum and Compact Steep Spectrum Radio Sources, I.A.G. Snellen, R.T. Schilizzi, H.J.A. Roettgering and M.N. Bremer eds, p. 142

O'Dea, C.P.: 1977 PASP in press

Owen, F.N., Eilek, J.A.: 1997 ApJ in press

Parma, P., de Ruiter, H.R., Fanti, C., Fanti, R.: 1986, A&AS64, 135

Readhead, A.C.S., Taylor G.B., Xu W., Pearson T.J.: 1996 ApJ460, 612

De Ruiter, H.R., Parma, P., Fanti, C., Fanti, R.: 1986, A&AS65, 111

Zabludoff, A.I., Geller, M.J., Huchra, J.P., Vogeley, M.S.: 1993 AJ106, 1273

Zensus J.A., Krichbaum, T.P., Lobanov, A.P.: 1995 Proc. Natl. Acad. Sci. USA 92, 11348